Electronic structure of Ga_{1−x}Mn_{x}As probed by four-wave mixing spectroscopy

M. Yildirim, S. March, R. Mathew, A. Gamouras, X. Liu, M. Dobrowolska, J. K. Furdyna, and K. C. Hall

Phys. Rev. B **84**, 121202 — Published 28 September 2011

DOI: 10.1103/PhysRevB.84.121202

Electronic structure of GaMnAs probed by four-wave mixing spectroscopy

M. Yildirim, S. March, R. Mathew, A. Gamouras, and K. C. Hall
Department of Physics and Atmospheric Science, Dalhousie University, Halifax, Nova Scotia B3H1Z9

X. Liu, M. Dobrowolska, and J. K. Furdyna
Department of Physics, University of Notre Dame, Notre Dame, IN 46556

Four-wave mixing experiments on GaMnAs indicate an increase in the optical response near the band gap with increasing Mn concentration. These findings are attributed to (s,p)-d hybridization, which leads to an enhancement in the density of states in the valence band. Our experiments show that the nonlinearity of the four-wave mixing technique provides a highly sensitive probe for Mn-related changes in the electronic structure of GaMnAs.

PACS numbers:

The III-V diluted magnetic semiconductors (DMS) exhibit a unique combination of semiconducting and ferromagnetic properties, offering the ability to control magnetic characteristics through modification of the carrier density.[1–6] This feature makes DMS materials of interest for developing semiconductor-based magneto-sensitive electronic and photonic devices that would exploit the spin degree of freedom.[7–16] Of the various DMS systems under study, GaMnAs has become the prototype material, with a considerable body of work over the past decade providing the foundation for a general picture of ferromagnetism in the III-V DMS. The ability to tailor the growth conditions and optimize post-growth annealing procedures has led to continual improvements in T_c for GaMnAs, reaching close to 200 K for Mn densities $\sim$10%.[17–19]

Despite these experimental advances, the theoretical understanding of the band structure and the underlying ferromagnetic interactions is still evolving, due in part to the complexity of treating (s,p)-d hybridization, localization effects and Coulomb interactions in the presence of disorder.[20–26] An ongoing debate concerning the location of the Fermi level, which may lie within the p-type valence band or within an impurity band with primarily d-character, has critical implications regarding the nature of transport and ferromagnetic order in this system.[22,24,25,27–32] Results of linear optical spectroscopy experiments have provided crucial input into this debate, as well as illuminating the fundamental properties of GaMnAs.[21,25,27–35] For instance, an absorption feature around 200 meV has provided a possible means to distinguish between valence band and impurity band models,[29] although sample-to-sample variations have complicated the interpretation of experimental results.[25] Magnetic circular dichroism and spectroscopic ellipsometry studies have also provided information regarding the sign (antiferromagnetic) and wavevector dependence of the p-d exchange interaction.[27,30,31,33–37]

Four-wave mixing spectroscopy provides another tool to investigate the electronic structure of GaMnAs. In this *nonlinear* optical technique, two incident optical pulses with wavevectors k_1 and k_2 together generate a third order nonlinear optical polarization that emits light with wavevector $2k_2$-k_1. The spectral content of this emission, together with its dependence on the time delay between the two exciting laser pulses, provides information regarding the density and nature of the electronic transitions, interactions within the excited carrier system, and the coherence decay time.[38–43] Four-wave mixing experiments are expected to provide a sensitive probe of Mn-related features in the electronic structure of III-Mn-V semiconductors, including the prevalence of defect-to-band transitions[27,33] and the influence of (s,p)-d hybridization on the valence states.[23,28] This sensitivity is tied to the nonlinearity of the technique, as the four-wave mixing polarization is proportional to the cube of the energy-dependent dipole matrix element. For example, four-wave mixing experiments have revealed the relative strength of exciton and band-to-band contributions in nonmagnetic Ge, GaAs, and InP.[39,40,43]

Here we report measurements of the four-wave mixing response of a family of $Ga_{1-x}Mn_xAs$ structures with x in the range 0 to 0.1%. The properties of GaMnAs in the low x limit have been the subject of several recent works as this regime provides a window into the electronic properties of Mn point defects and the effects of (s,p)-d hybridization.[22,23,44–51] Our experiments indicate a strong increase in the optical response above the fundamental band gap with the addition of Mn with x as low as 0.005 %. We attribute this observation to an increase in the density of states near the valence band edge caused by hybridization between the d-levels of the Mn_{Ga} and the p-states of the host GaAs crystal, as predicted theoretically.[23] Mn-induced states near the valence band maximum were seen in angle-resolved photoemission,[54] however the energy resolution was relatively low ($\sim$100 meV). A broad increase in the optical response of GaMnAs in the vicinity of the band gap with the addition of Mn has also been observed in absorption and ellipsometry experiments,[27,33] although a strong absorption tail characteristic of low-temperature grown GaAs and GaMnAs masks any Mn-related features near the fundamental band gap in linear spectroscopy.[53]

Our experiments indicate that the absorption tail provides only a weak contribution to the four-wave mixing spectrum due to the difference in the dipole transitions strengths for defect-to-band and band-to-band absorption channels. This sensitivity, which is afforded by the nonlinearity of the technique used here, has allowed us to observe clear optical signatures of (s,p)-d hybridization, providing new insight into the electronic structure of GaMnAs.

The samples for this work were grown by molecular beam epitaxy and consist of 800 nm of $Ga_{1-x}Mn_xAs$ grown on top of a 175 nm $Al_{0.27}Ga_{0.73}As$ stop etch layer on a semi-insulating GaAs substrate. The samples were glued face down to c-cut sapphire windows and the substrates were removed using mechanical polishing followed by wet etching in order to enable experiments in the transmission geometry. The substrate growth temperature and Mn concentration for the samples studied here are listed in Table 1. The Mn content for the single GaMnAs sample grown at 600 ^{0}C is only an estimate as the Mn will exist in a combination of Mn point defects and precipitates. The thickness of the GaMnAs layer was chosen to provide sufficient four-wave mixing signal without introducing propagation effects.

The linear absorption spectra for the samples described in Table 1 are shown in Fig. 1(a). These measurements were made using a continuous-wave white light source (Ocean Optics LS-1). The absorption coefficient was extracted from the raw transmission data using a self-consistent model incorporating multiple reflections in the sample layer. Weak residual Fabry Perot oscillations persist for low photon energies, but do not obscure the dominant trends in Fig. 1(a). The two samples grown at 600 ^{0}C exhibit a clear excitonic peak and a sharp band edge response, as expected since the elevated temperature of the substrate during growth results in a low density of defects. The exciton absorption peak in HT GaMnAs is observed to be red shifted by 2.5 meV relative to HT GaAs. We attribute this shift to the dominant emission of excitons bound to Mn-related defects. In contrast, no exciton is visible in any of the low-temperature-grown samples, and there is a substantial absorption below the band gap. Smearing of the band edge features with low temperature growth is due to excess arsenic, an effect that has been well studied in LT GaAs.[53,55] Excess arsenic leads to the formation of band tail states associated with local potential fluctuations[55,56] and a deep donor band due to As_{Ga} antisite defects,[28,53] both of which lead to absorption pathways for photon energies below the band gap of HT GaAs. The absorption tail is largest in the LT GaAs sample, as expected because the As_{Ga} mid-gap donor band will be occupied, leading to strong linear absorption from the mid-gap band to the conduction band. In the LT GaMnAs samples, compensation due to the Mn_{Ga} acceptors reduces this absorption channel relative to LT GaAs.[28] For increasing Mn concentration, the absorption tail increases in the LT GaMnAs samples, reflecting the increasing degree of Mn-related local potential fluctuations and associated band tailing.

Spectrally-resolved four-wave mixing experiments were carried out in the two-pulse self-diffraction geometry, as shown schematically in Fig. 1(b). The optical source is a mode-locked Ti:Sapphire oscillator, producing pulses with a center photon energy of 1.55 eV. A prism compressor was integrated into the optical setup to compensate for dispersion, providing a pulse duration at the sample position of 20 fs, detected using the zero background autocorrelation signal at an equivalent focus. The laser pulse spectrum, which is broad enough to overlap the band edge region as well as the absorption tail, is shown in Fig. 1(a) by the filled circles. The four-wave mixing signal was spectrally resolved using a monochromator and detected using a photomultiplier tube. The spectral sensitivity of the entire setup was calibrated using the white light source. The pulse delay (τ) was varied using the rapid scan approach, with a retroreflector mounted to the cone of a woofer speaker. The zero delay position was determined by simultaneously detecting the four-wave mixing signal along $2k_1$-k_2 and $2k_2$-k_1, which form a mirror image about $\tau = 0$.[40] The density of electron-hole pairs excited by the laser pulse was estimated using the incident and transmitted powers through the sample to be 6×10^{16} cm^{-3}. The optical density of the samples is 0.2, indicating that propagation effects may be neglected.[57] The sample was held at 10 K in a liquid helium flow-through cryostat for all measurements.

The results of four-wave mixing measurements on the HT GaAs reference sample are shown in Fig. 2(a). The signal is strongly dominated by the optical response of the exciton, which exhibits a spectrally narrow peak centered at zero time delay. This signal decays very rapidly versus delay, with a decay time that is comparable to the laser pulse duration. A weak response from the valence to conduction band transitions is also observed on the high energy side of the exciton. The continuum response peaks at positive time delay and decays more slowly than the exciton response. These general characteristics were observed in earlier experiments on high-temperature-grown GaAs, Ge and InP.[40,58,59] The interband response is characteristic of an inhomogeneously-broadened transition,[60,61] while the exciton signal is dominated by an interaction-induced nonlinearity related to exciton-carrier scattering.[41–43] As seen in Fig. 2(b), HT GaMnAs exhibits a similar four-wave mixing response to HT GaAs, reflecting the clean band structure in this sample. Faster dephasing kinetics in the HT GaMnAs sample causes the interband contribution to peak closer to zero delay than in HT GaAs,[60] likely reflecting carrier scattering with the Mn impurities.[62] The signal characteristics change qualitatively when the structure is grown at low temperature: For all of the samples in Fig. 2(c)-Fig. 2(f), an additional signal component appears below the band gap. With increasing x, the four-wave mixing response of LT-GaMnAs progressively broadens to the high energy side. Measurements for a range of excited carrier density indicate some evidence of saturation at the exciton in the HT-GaAs response, likely reflecting screening of the exciton-carrier scattering coefficient.[41] For the continuum response of HT GaAs at higher photon energies, and for data at all energies in all other samples, the power dependence indicates that the nonlinear response is in the $\chi^{(3)}$ regime.

These trends may be seen more clearly in Fig. 3, which shows the four-wave mixing spectrum at zero delay. The sharp peak at the exciton is dominant in the optical response for HT GaAs and HT GaMnAs. A 2.5 meV red shift is observed for the HT GaMnAs exciton response, consistent with the linear absorption data in Fig. 1(a). The exciton peak in HT GaMnAs is also broader than that in HT GaAs (11 meV compared to 8 meV in HT GaAs), consistent with an increased dephasing rate due to scattering with Mn-related defects. Since the peak of the signal due to the interband transitions occurs closer to zero delay in the HT GaMnAs sample than in HT GaAs, it may be seen in the zero delay spectrum for HT GaMnAs as the small peak on the high energy side of the exciton. A low energy shoulder appears in all of the samples grown at low temperatures, with a similar spectral shape and strength across the samples. The four-wave mixing response remains peaked at the exciton energy for both the LT GaAs sample and the sample with the lowest Mn concentration ($x = 0.005$ %), although the latter signal is considerably broader and assymetric to the high-energy side. For higher x, the peak broadens further, and the peak center shifts to higher photon energies.

As the low energy shoulder is present for all samples grown at low temperature, it is not tied to the Mn doping. We attribute this shoulder to the nonlinear optical response of band tail states induced by local potential fluctuations, as the associated optical transitions are expected to be similar in strength to the interband transitions.[55] Optical transitions between the As_{Ga} mid-gap donor band and the conduction band provide an additional absorption channel for the photon energies investigated here, however these transitions are expected to generate a broad, featureless response, with a spectral shape similar to the laser spectrum, in contrast to the observations in Fig. 3. The absence of a significant four-wave mixing response associated with these defect-to-band transitions indicates that the matrix element of the dipole operator associated with these transitions is small compared to that for the interband transitions. This conclusion is consistent with findings in p-type GaAs, where no response associated with the acceptor-deionization band was observed even up to 120 K.[63] Differences in transition strength for various signal contributions are amplified in nonlinear optical experiments like four-wave mixing spectroscopy because the source polarization in the experiments is proportional to the cube of the dipole matrix element for the transition.

The 3d orbitals of the Mn_{Ga} substitutional impurity hybridize with the p orbitals of the As atoms. This (s,p)-d hybridization is the origin of the strong exchange coupling between the hole and the Mn local moments responsible for ferromagnetic order. The bound Mn acceptor level located 110 meV above the valence band edge has been well characterized using infrared absorption spectroscopy.[46,64] Much less is known about the influence of (s,p)-d hybridization on the delocalized valence states. In angle-resolved photoemission experiments, an increase in the emission intensity was observed for energies between the Fermi energy and 0.5 eV below.[54] This was attributed to states induced by Mn near the valence band maximum, although the energy resolution in those experiments was limited to ∼100 meV. Using a local tight binding model, Tang and Flatté predicted a strong enhancement in the valence band density of states due to hybridization extending from the band edge to more than 1 eV below.[23] The blue shift and broadening we observe is consistent with an increased optical response associated with the interband transitions induced by an increase in the valence band density of states. We therefore attribute these observations to signatures of (s,p)-d hybridization. No such signatures have been observed in linear absorption experiments due to the dominant absorption contributions of band tail states and transitions involving the As_{Ga} impurity band.[33] Band edge smearing prevented even the observation of a critical point at the band gap in GaMnAs in spectroscopic ellipsometry experiments.[27] The contrast in sensitivity of linear and nonlinear spectroscopy is evident from a comparison of the evolution of the spectrum with x in Fig. 1(a) and Fig. 3: The four-wave mixing signal exhibits a gradual evolution as x increases, whereas no qualitative difference is observed in the linear absorption data for any of the low temperature grown samples. Our ability to observe clear effects of (s,p)-d hybridization in four-wave mixing experiments is tied to the nonlinearity of the technique and the associated enhancement in sensitivity to fine features in the optical joint density of states.

In conclusion, we have studied the nonlinear optical response of GaMnAs using femtosecond four-wave mixing spectroscopy. Our experiments indicate a distinct reshaping of the four-wave mixing spectrum with the addition of Mn, corresponding to an increase in the optical response above the band gap. We attribute these observations to the effects of (s,p)-d hybridization on the valence band states. Our results show that four-wave mixing techniques provide increased sensitivity to Mn-related changes in the electronic structure for states in the vicinity of the band gap when compared to traditional linear spectroscopy experiments. Our findings provide new insight into the fundamental properties of GaMnAs.

This research is supported by the Canada Foundation for Innovation, the Natural Sciences and Engineering Research Council of Canada, Lockheed Martin Corporation, the Canada Research Chairs Program, and the National Science Foundation (Grant DMR10-05851).

References

[1] H. Ohno, D. Chiba, F. Matsukura, T. Omiya, E. Abe, T. Dietl, Y. Ohno, and K. Ohtani, Nature **408**, 944 (2000).
[2] D. Chiba, M. Yamanouchi, F. Matsukura, and H. Ohno, Science **301**, 943 (2003).
[3] S. Koshihara, A. Oiwa, M. Hirasawa, S. Katsumoto, Y. Iye, C. Urano, H. Takagi, and H. Munekata, Phys. Rev. Lett. **78**, 4617 (1997).
[4] A. Oiwa, T. Slupinski, and H. Munekata, Appl. Phys. Lett. **78**, 518 (2001).
[5] K. C. Hall, J. P. Zahn, A. Gamouras, S. March, J. L. Robb, X. Liu, and J. K. Furdyna, Appl. Phys. Lett. **93**, 032504 (2008).
[6] J. P. Zahn, A. Gamouras, S. March, X. Liu, J. K. Furdyna, and K. C. Hall, J. Appl. Phys. **107**, 033908 (2010).
[7] S. A. Wolf, D. D. Awschalom, R. A. Buhrman, J. M. Daughton, S. von Molnar, M. L. Roukes, A. Y. Chtchelkanova, and D. M. Treger, Science **294**, 1488 (2001).
[8] *Semiconductor Spintronics and Quantum Computation*, edited by D. D. Awschalom, D. Loss, and N. Samarth (Springer-Verlag, Berlin Heidelberg New York, 2002).
[9] S. Datta and B. Das, Appl. Phys. Lett. **56**, 665 (1990).
[10] K. C. Hall, W. H. Lau, K. Gündoğdu, M. E. Flatté, and T. F. Boggess, Appl. Phys. Lett. **83**, 2937 (2003).
[11] K. C. Hall and M. E. Flatté, Appl. Phys. Lett. **88**, 162503 (2006).
[12] T. Kuroiwa, T. Yasuda, F. Matsukura, A. Shen, Y. Ohno, Y. Segawa, H. Ohno, Electron. Lett. **34**, 190 (1998).
[13] K. Onodera, T. Masumoto, and M. Kimura, Electron. Lett. **30**, 1954 (1994).
[14] Y. Nishikawa, A. Tackeuchi, S. Nakamura, S. Muto, and N, Yokoyama, Appl. Phys. Lett. **66**, 839 (1995).
[15] K. C. Hall, S. W. Leonard, H. M. van Driel, A. R. Kost, E. Selvig, and D. H. Chow, Appl. Phys. Lett. **75**, 4156 (1999).
[16] J. Rudolph, D. Hägele, H. M. Gibbs, G. Khitrova, M. Oestreich, Appl. Phys. Lett. **82**, 4516 (2003).
[17] V. Novák, K. Olejník, J. Wunderlich, M. Cukr, K. Výborný, A. W. Rushforth, K. W. Edmonds, R. P. Campion, B. L. Gallagher, Jairo Sinova, and T. Jungwirth, Phys. Rev. Lett. **101**, 077201 (2008).
[18] P. Vašek, P. Svoboda, V. Novák, M. Cukr, Z. Výborný, V. Jurka, J. Stuchlík, M. Orlita, and D. K. Maude, J. Supercond. Nov. Magn. **23**, 1161 (2010).
[19] L. Chen, X. Yang, F. Yang, J. Zhao, J. Misuraca, P. Xiong, and S. von Molnár, Nano Letters, published online (2011).
[20] J. Mašek, F. Máca, J. Kudrnovský, O. Makarovsky, L. Eaves, R. P. Campion, K. W. Edmonds, A. W. Rushforth, C. T. Foxon, B. L. Gallagher, V. Novák, J. Sinova, and T. Jungwirth, Phys. Rev. Lett. **105**, 227202 (2010).
[21] S. Katsumoto, T. Hayashi, Y. Hashimoto, Y. Iye, Y. Ishiwata, M. Watanabe, R. Eguchi, T. Takeuchi, Y. Harada, S. Shin, K. Hirakawa, Mater. Sci. Eng. B **84**, 88 (2001).
[22] B. L. Sheu, R. C. Myers, J.-M. Tang, N. Samarth, D. D. Awschalom, P. Schiffer, and M. E. Flatté, Phys. Rev. Lett. **99**, 227205 (2007).
[23] J.-M. Tang and M. E. Flatté, Phys Rev. Lett. **92**, 047201 (2004).
[24] S. Ohya, K. Takata, and M. Tanaka, Nature Physics 7, 342 (2011).
[25] T. Jungwirth, P. Horodyská, N. Tesařová, P. Němec, J. Šubrt, P. Malý, P. Kužel, C. Kadlec, J. Mašek, I. Němec, M. Orlita, V. Novák, K. Olejník, Z. Šobáň, P. Vašek, P. Svoboda, and J. Sinova, Phys. Rev. Lett. **105**, 227201 (2010).
[26] K. S. Burch, D. D. Awschalom, and D. N. Basov, J. Magn. Magn. Mater. **320**, 3207 (2008).
[27] K. S. Burch, J. Stephens, R. K. Kawakami, D. D. Awschalom, and D. N. Basov, Phys. Rev. B **70**, 205208 (2004).
[28] E. J. Singley, K. S. Burch, R. Kawakami, J. Stephens, D. D. Awschalom, D. N. Basov, Phys. Rev. B **68**, 165204 (2003).
[29] K. S. Burch, D. B. Shrekenhamer, E. J. Singley, J. Stephens, B. L. Sheu, R. K. Kawakami, P. Schiffer, N. Samarth, D. D. Awschalom, and D. N. Basov, Phys. Rev. Lett. **97**, 087208 (2006).
[30] G. Acbas, M.-H. Kim, M. Cukr, V. Novák, M. A. Scarpulla, O. D. Dubon, T. Jungwirth, Jairo Sinova, and J. Cerne, Phys. Rev. Lett. 103, 137201 (2009).
[31] B. Beschoten, P. A. Crowell, I. Malajovich, D. D. Awschalom, F. Matsukura, A. Shen, and H. Ohno, Phys. Rev. Lett. **83**, 3073 (1999).
[32] T. Dietl, H. Ohno and F. Matsukura, Phys. Rev. B **63**, 195205 (2001).
[33] J. Szczytko, W. Mac, and A. Twardowski, F. Matsukura and H. Ohno, Phys. Rev. B **59**, 12935 (1999).
[34] J.-M. Tang and M. E. Flatté, Phys. Rev. Lett. **101**, 157203 (2008).
[35] M. Berciu, R. Chakarvorty, Y. Y. Zhou, M. T. Alam, K. Traudt, R. Jakiela, A. Barcz, T. Wojtowicz, X. Liu, J. K. Furdyna, and M. Dobrowolska, Phys. Rev. Lett. **102**, 247202 (2009).
[36] K. Ando, Science **312**, 1883 (2006)
[37] K. Ando, T. Hayashi, M. Tanaka and A. Twardowski, J. Appl. Phys. **83**, 6548 (1998)
[38] K. Leo, M. Wegener, J. Shah, D. S. Chemla, E. O. Göbel, T. C. Damen, S. Schmitt-Rink, and W. Schäfer, Phys. Rev. Lett. **65**, 1340 (1990).
[39] D.-S. Kim, J. Shah, J. E. Cunningham, T. C. Damen, W. Schäfer, M. Hartmann, and S. Schmitt-Rink, Phys. Rev. Lett. **68**, 1006 (1992).
[40] T. Rappen, U. Peter, M. Wegener, and W. Schäfer, Phys. Rev. B **48**, 4879 (1993).
[41] S. T. Cundiff, M. Koch, W. H. Knox, J. Shah, and W. Stolz, Phys. Rev. Lett. **77**, 1107 (1996).
[42] K. El Sayed, D. Birkedal, V. G. Lyssenko, and J. M. Hvam, Phys. Rev. B **55**, 2456 (1997).
[43] K. C. Hall, G. R. Allan, H. M. van Driel, T. Krivosheeva, and W. Pötz, Phys. Rev. B **65**, 201201(R) (2002).

[44] M. Poggio, R. C. Myers, N. P. Stern, A. C. Gossard, and D. D. Awschalom, Phys. Rev. B **72**, 235313 (2005).
[45] R. C. Myers, M. Poggio, N. P. Stern, A. C. Gossard, and D. D. Awschalom, Phys. Rev. Lett. **95**, 017204 (2005).
[46] R. A. Chapman and W. G. Hutchinson, Phys. Rev. Lett. **18**, 443 (1967).
[47] A. Kaminski and S. Das Sarma, Phys. Rev. Lett. **88**, 247202 (2002).
[48] Steven C. Erwin and A. G. Petukhov, Phys. Rev. Lett. **89**, 227201 (2002).
[49] G. A. Fiete, G. Zaránd, and Kedar Damle, Phys. Rev. Lett. **91**, 097202 (2003).
[50] S.-R. E. Yang, and A. H. MacDonald, Phys. Rev. B **67**, 155202 (2003).
[51] M. Berciu and R. N. Bhatt, Phys. Rev. Lett. **87**, 107203 (2001).
[52] R. Chakarvorty, Y.-Y. Zhou, Y.-J. Cho, X. Liu, R. Jakiela, A. Barcz, J. K. Furdyna, and M. Dobrowolska, IEEE Trans. on Magn. **43**, 3031 (2007).
[53] D. Streb, M. Ruff, S. U. Dankowski, P. Kiesel, M. Kneissl, S. Malzer, U. D. Keil, and G. H. Döhler, J. Vac. Sci. Technol. B **14**, 2275 (1996).
[54] J. Okabayashi, A. Kimura, O. Rader, T. Mizokawa, A. Fujimori, T. Hayashi, and M. Tanaka, Phys. Rev. B **64**, 125304 (2001).
[55] G. Segschneider, T. Dekorsy, H. Kurz, R. Hey, and K. Ploog, Appl. Phys. Lett. **71**, 2779 (1997).
[56] Sajeev John, Costas Soukoulis, Morrel H. Cohen and E. N. Economou, Phys. Rev. Lett. **57**, 1777 (1986).
[57] L. Bányai, D. B. Tran Thoai, E. Reitsamer, H. Haug, D. Steinbach, M. U. Wehner, M. Wegener, T. Marschner and W. Stolz, Phys. Rev. Lett. **75**, 2188 (1995).
[58] A. Lohner, K. Rick, P. Leisching, A. Leitenstorfer, T. Elsaesser, T. Kuhn, F. Rossi, and W. Stolz, Phys. Rev. Lett. **71**, 77 (1993).
[59] G. R. Allan and H. M. van Driel, Phys. Rev. B **59**, 15740 (1999).
[60] T. Yajima and Y. Taira, J. Phys. Soc. Jpn. **47**, 1620 (1979).
[61] T. Zhang, I. Kuznetsova, T. Meier, X. Li, R. P. Mirin, P. Thomas, and S. T. Cundiff, PNAS **104**, 14227 (2007).
[62] S. T. Cundiff, R. Hellmann, M. Koch, G. Mackh, A. Waag, G. Landwehr, W. H. Knox, E. O. Göbel, J. Opt. Soc. Am. B **13**, 1263 (1996).
[63] A. Leitenstorfer, A. Lohner, K. Rick, and P. Leisching, T. Elsaesser, T. Kuhn, F Rossi, W. Stolz, and K. Ploog, Phys. Rev. B **49**, 16372 (1994).
[64] M. Linnarsson, E. Janzén, B. Monemar, M. Kleverman and A. Thilderkvist, Phys. Rev. B **55**, 6938 (1997).

TABLE I: Summary of characteristics of $Ga_{1-x}Mn_xAs$ samples for four-wave mixing experiments. HT (LT) indicates growth at high (low) substrate temperature. The Mn concentration was determined by secondary ion mass spectrometry.[52] *The Mn content in the HT GaMnAs sample is an upper estimate only, as discussed in the text.

Sample	Growth Temperature	x(%)
HT GaAs	600	0
LT GaAs	250	0
LT GaMnAs	250	0.005
LT GaMnAs	250	0.045
LT GaMnAs	250	0.100
HT GaMnAs*	600	0.100

Figure Captions

Fig. 1: Results of linear transmission experiments at 10 K. The laser spectrum for the 20 fs pulses used in the four-wave mixing experiments is indicated by the filled circles. (b) Schematic diagram of the four-wave mixing apparatus.

Fig. 2: Results of spectrally-resolved four-wave mixing experiments at 10 K on the samples described in Table 1. The contour scale indicates the amplitude of the four-wave mixing signal, which is equal for all LT samples within the experimental uncertainty. The maximum contour scale for the two HT samples is much larger: by a factor of 20 for HT GaAs in (a) and by a factor of 12 for HT GaMnAs in (b).

Fig. 3: Top panel: four-wave mixing spectra at 10 K taken at zero pulse delay. Bottom panel: the laser excitation spectrum.

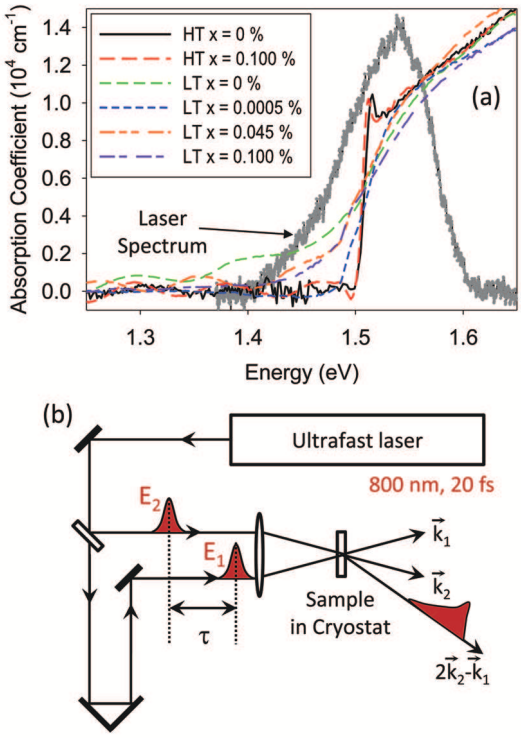

FIG. 1: Yildirim et al.

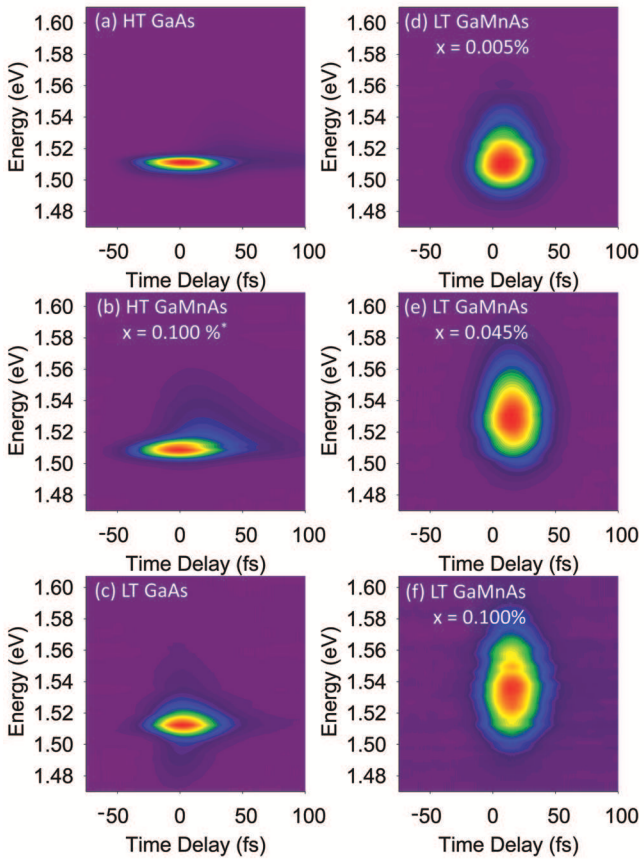

FIG. 2: Yildirim et al.

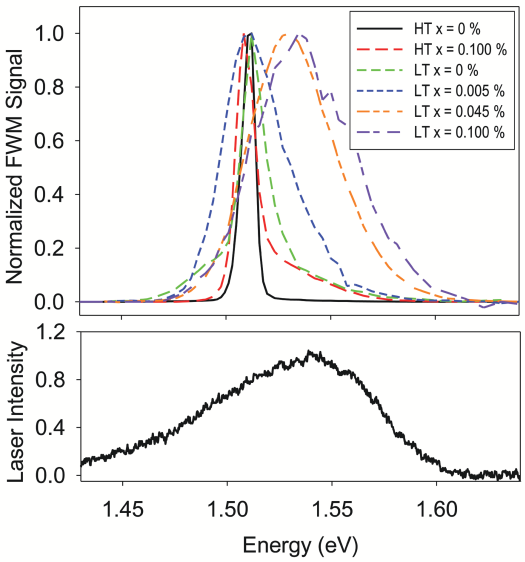

FIG. 3: Yildirim et al.